MASTER THESIS

ACTUATION, CONTROL AND LOCALIZATION OF UNTETHERED MAGNETIC ROBOTS

RITWIK AVANEESH

FACULTY OF ELECTRICAL ENGINEERING, COMPUTER SCIENCE AND MATHEMATICS (EEMCS)

DEPARTMENT OF ELECTRICAL ENGINEERING

EXAMINATION COMMITTEE
DR. ISLAM S. M. KHALIL
PROF. DR. SARTHAK MISRA
DR. MOMEN ABAYAZID

DOCUMENT NUMBER
BE-856

JUNE 2, 2022

UNIVERSITY OF TWENTE.

Thesis submitted by Ritwik Avaneesh

under the supervision of Dr. Islam S. M. Khalil,

Prof. Dr. Sarthak Misra and,
Dr. Momen Abayazid
in order to fulfill the necessary requirements to obtain a Master's degree in

Electrical Engineering at the University of Twente

and defended on

Thursday, June 2, 2022

Part of this work has been published at the International Conference on Intelligent Robots and Systems (IROS 2021): R. Avaneesh, R. Venezian, S. Misra and I. S. M. Khalil, "Open-Loop Magnetic Actuation of Helical Microrobots using Position-Constrained Rotating Dipole Field"

Acknowledgement

This thesis is the culmination of a years worth of work at the Surgical Robotics Laboratory (SRL), Uinversity of Twente, to graduate with a Master's degree in Electrical Engineering. During my research I have gathered key insights into the world of magnetics and unthered mobile robots. My work has helped me learn about designing, modelling and practical implementation of magnetic actuation systems for wireless control and localization of tetherless magnetic robots and eventually applying this acquired knowledge onto real world experimental setups. I wish to thank a number of people without whom this work could not have been possible, fellow colleagues with whom I have discussed about our projects, and my parents who have supported me throughout this journey.

First and foremost, I want to thank Dr. Islam S.M Khalil and Prof. Dr. Sarthak Misra. Dr. Islam S.M Khalil has been my daily supervisor for my entire duration working at SRL. He has provided me with invaluable guidance and support from day one. During our interactions, we had many fruitful discussions and I have learnt a lot from him. He constantly motivated me and provided me with clarity and sound advise while I was undertaking my research. In addition he has had a large hand in getting our research papers ready, one of which has been published in International Conference on Intelligent Robots and Systems (IROS 2021) and are currently working on the submission of our second paper. I want to thank Prof. Dr. Sarthak Misra firstly, for being part of my graduation committee and providing me the opportunity to carry out my internship and thesis research at SRL and secondly for giving comments and indications to all the students during the SRL meetings.

I want to express special thanks to Dr. M. Abayazid for being the external member of my graduation committe. In addition, I want to thank my teammate Roberto Venezian and my colleagues Mina Micheal, Mert kaya, Zhengya Zhang, Dr. Sumit Mohanty, Dr. Jakub Sikorski and Dr. Christoff M. Heunis for being open to discussions and helping me out when in need. Finally, a warm thanks to my parents for all the support throughout this project, especially during the most stressful periods.

Ritwik Avaneesh
June 2, 2022

Abstract

Over the past two decades there has been a paradigm shift in the field of small scale mobile magnetic robots. various research groups have show keen interest in remote manipulation, wireless actuation and control of these untethered magnetic robots. The potential impact of these robots in the field of healthcare and bio-engineering applications could be unprecedented in the near future. As an alternative to existing tethered medical devices such as flexible endoscopes and catheters, these wireless magnetic robots could access complex and small regions of the human body such as gastrointestinal tract, spinal cord, brain, blood capillaries, and inside the eye while being minimally invasive and could even access sub-millimeter size regions inside the human body, which have not been possible to access currently with any medical technology. As a part of this thesis, we investigate the underlying actuation principles to control these wireless magnetic robots and present a very novel noninvasive localization method to estimate the position of these robots. The thesis is divided into two parts, the first half deals with control of tetherless magnetically actuated helical robots using rotating dipole fields. we study the open-loop response of helical robots (in viscous fluids characterized by low Reynolds numbers) in the presence of position constraints on the actuating rotating permanent magnet. We first derive a mapping between the space of the manipulator's joints, the produced magnetic fields in three-dimensional space, and the translational and rotational velocities of the helical robot. Then, we constrain the 3D position of the rotating dipole field and predict the response of the helical robot by controlling its angular velocity using the constrained mapping. We demonstrate open-loop control and gravity compensation of the robot using the angular velocities of the actuating permanent magnet while enforcing constraints on the end-effector position. In the second half of the thesis, we theoretically and experimentally investigate a novel eye-in-hand noninvasive magnetic localization and actuation method to determine the position of magnetic milli-rollers via permanent magnetic coupling using the detected disturbance torque on the rotating permanent magnet. We first model the dynamics of the rotating dipole field that is controlled using a serial manipulator to actuate a tetherless milli-roller inside a fluid-filled lumen and design an observer to determine the magnetic torque caused by its motion with respect to the rotating permanent magnet. Then we use the point dipole approximation of the magnetic coupling and the kinematics of the permanent-magnet robotic system to estimate the position of the milli-roller.

Contents

Page No.

Chapter 1: An Introduction to Magnetic Actuation and Control of Untethered Magnetic Robots

I. BACKGROUND

Small scale robots have attracted increasing attention in recent years, mainly because of their potential applications in medical and bioengineering [1], [2]. These robots are controllable devices with size ranging from micro-meters to millimeters [3]. Due their small scale, these robots can access complex and narrow regions of the human body in a minimally invasive manner. The effectiveness of these devices has been investigated to perform a wide range of non-trivial tasks such as biopsy [4], drug delivery [5], diagnostic sensing [6], medical examination and even mechanical rubbing of blood clots [7], [8].

Owing to their small size, the developed tiny robots are expected to reshape medical diagnosis and treatment with minimally invasive procedures. However, integrating conventional on-board components (e.g., actuators, processors, and power sources) becomes very difficult due to the restricted volume, especially for sub-millimeter robots. To date, diverse strategies have been proposed, such as chemical, optical, ultrasonic, electrostatic, and magnetic actuation. Among these, magnetic actuation is one of the preferred strategies because it is transparent and relatively safe to biological tissues and it has good controllability [9], [10]. Even for robots in millimeter scales, motivated by the simultaneous pursuit of good maneuverability and minimal invasion, the contradiction between active modality and small size always exists for the on-board design, and using off board magnetic actuation has become a feasible solution [11], [12]. Therefore, magnetic small scale robots have been widely developed. Externally-generated magnetic fields have been shown to be capable of driving magnetic devices of many different sizes from microrobots [13], [14], to centimeter-scale medical devices including capsule endoscopes [15], [16], ophthalmic implements [17], steerable needles [18] and catheters [19], [20]. These magnetic tools can be considered the end-effectors of a larger robotic system consisting of the external field source, the camera or other feedback device, and the computer that controls the tool's motion.

In general, magnet actuation systems must be able to position or orient the magnetic tool with a high level of precision. The orientation of a magnetic tool can be adjusted by applying a magnetic field, which interacts with the moment of the magnetic tool to produce a torque. Similarly, the position of a magnetic tool can be adjusted by applying a magnetic field gradient (i.e. a field that varies with distance) that interacts with the tool moment to produce a force. An implement containing a single magnetic dipole can be driven with a maximum of 5 DOF, consisting of 3 DOF for translational and 2 DOF for rotational (the third rotational DOF requires a torque to be applied about the magnetization axis which is not possible for a single dipole). Existing magnetic control systems can be divided into two broad categories based on the field source: 1) electromagnets that produce a field when current is applied to a coiled wire and 2) permanent magnets that produce a constant field due to the alignment of the domains in their internal micro-crystalline structure.

There are three types of coils implemented in electromagnetic systems. Helmholtz style coils produce a uniform field, Maxwell style coils produce a fixed field gradient, and coils that produce an approximate dipole shaped field. Helmholtz coil setup can generate various magnetic fields adapted for the motion control of different microrobots: for example, a square wave oscillating magnetic field for actuating a jellyfish-like swimming microrobot [21], an on/off magnetic field for the motion control of flexible metal nanowire motors [22] or for a magnetic mite (MagMite) [23] and a conical magnetic field to decrease the off-axis motion of helical microrobots [24]. Yesin et al. [25] developed a combination of a coaxial pair of Helmholtz coils and Maxwell coils to control an elliptical-shaped microrobot . The combination of coils is mounted on a rotating stage, so that it can rotate around the workspace to control the orientation of the magnetic field. Therefore, the setup enables 3 DOF, including 1 DOF for rotation and 2 DOF for translation. The direction of the magnetic field is changed by a mechanical method, which is not simultaneous. The combination with two pairs of Maxwell coils and two pairs of Helmholtz coils also enables a 3 DOF control of the microrobots with a simultaneous change of the magnetic direction controlled by currents [26], [27].

Electromagnetic systems have a comprehensive ability of magnetic field generation, on/off manipulability of magnetic field and employ simple current control strategy. However, they are difficult to scale up to the size required for in vivo medical applications. A reliance on uniform fields requires that the robot be located in the small central region of the system's workspace. However, there are no locations in the human body that can be described as being "at the centre" in any reasonable sense; the human body is geometrically too complex. To overcome these issues Abbott et al. proposed the use of nonuniform magnetic fields emanating from a single rotating permanent magnet for control of such untethered magnetic robots [28], [29]. Allowing non uniform magnetic fields makes it possible to place the magnet closer to the

patient, which permits the use of smaller and less-expensive systems. The use of nonuniform fields results in undesirable field gradient forces, making control more challenging, but may ultimately result in superior systems in terms of size and cost compared to using uniform fields.

Systems utilising permanent magnets can be divided into two general categories: 1) systems composed of one or more rotating magnets that are used to generate a rotating magnetic field and 2) systems containing a single permanent magnet that is manipulated in order to control the position and orientation of a capsule endoscope within the body.

A commonly proposed use for permanent magnetic actuation systems is the production of a rotating magnetic field in order to drive micro or milli-scale helical swimmers [30] [31] and rolling robots. Helical swimmers are spiral-shaped devices that can be driven through a viscous fluid environment in 3D by applying a rotating magnetic field perpendicularly to the desired direction of movement. Rolling robots are typically cube or spherical shaped and can be rolled end-over-end on a horizontal surface by applying a rotating magnetic field that is parallel to the desired motion.

II. Magnetic Actuation and Magnetic Fields

In this section, we discuss the principles governing the actuation of small scale magnetic robots and briefly introduce the source of magnetic field generation, which include permanent magnets and electromagnets.

A. Principle for Magnetic Actuation

The principle of magnetic actuation is to propel these untethered small scale robots typically consisting of a rigidly attached magnetic body, by imparting magnetic force and/or torque on them through remotely applied external magnetic fields. Since, no currents exist in the region of interest the quasistatic magnetic field can be described by Maxwell's equation as

$$\nabla \cdot \mathbf{B} = 0 \tag{1}$$

$$\nabla \times \mathbf{B} = 0 \tag{2}$$

Where $\mathbf{B} \in \mathbb{R}^3$ is the applied external magnetic field and ∇ is the gradient operator. The equation implies that the gradient matrix is symmetric and traceless. A magnetic torque $\boldsymbol{\tau}$ acts on the magnetic dipole $\mathbf{m} \in \mathbb{R}^3$ of the robot when it is misaligned with the orientation of the magnetic field, given by

$$\boldsymbol{\tau} = \mathbf{m} \times \mathbf{B} = \begin{pmatrix} 0 & B_z & -B_y \\ B_z & 0 & B_x \\ B_y & -B_x & 0 \end{pmatrix} \begin{pmatrix} m_x \\ m_y \\ m_z \end{pmatrix} \tag{3}$$

Moreover, the robot experiences a magnetic force $\mathbf{f}$, when placed in a non uniform magnetic field, given by

$$\mathbf{f} = (\mathbf{m} \cdot \nabla)\mathbf{B} = \begin{pmatrix} \frac{\partial B_x}{\partial x} & \frac{\partial B_x}{\partial y} & \frac{\partial B_x}{\partial z} \\ \frac{\partial B_x}{\partial y} & \frac{\partial B_y}{\partial y} & \frac{\partial B_y}{\partial z} \\ \frac{\partial B_x}{\partial z} & \frac{\partial B_y}{\partial z} & -(\frac{\partial B_x}{\partial x} + \frac{\partial B_y}{\partial y}) \end{pmatrix} \begin{pmatrix} m_x \\ m_y \\ m_z \end{pmatrix} \tag{4}$$

These two effects can separately or simultaneously be used to actuate the magnetic robot, therefore allowing upto 6-DOF motion control.

B. Generation of Magnetic Field

1) Electromagnets: Electromagnets are capable of producing current dependent magnetic fields that can be controlled. Uniform magnetic fields and uniform magnetic gradients can be generated through these specialised coil pairs, namely Helmholtz coil and Maxwell coil.

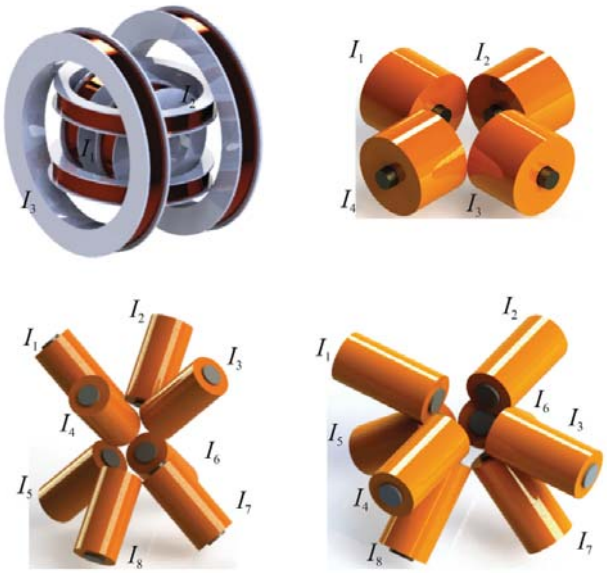

Fig. 1: Electromagnetic-based manipulation systems are used to actuate small scale untethered magnetic robots near the common center of the coils. The current inputs $(I_1, ..., I_n)$ are applied such that generated dynamic magnetic field rotates about an axis of rotation that is aligned with the desired reference trajectory. The configurations of multiple electromagnetic coils enable the field to oscillate in 3-D space and are designed specifically to work based on the environment and the intended application [32].

A uniform magnetic field can be generated by a Helmholtz coil pair, which are made up of two identical circular coils aligned on the same axis and separated by a distance equal to the radius of the coil with identical currents passing in the same direction. A 3D Helmholtz coil system consists of three orthogonally arranged Helmholtz coil pairs, this arrangement of coils can generate a uniform rotating magnetic field $\mathbf{B}_{\perp n}$ around any axis n in the 3D space by the modulation of currents passing through the coils. The magnetic field is expressed as follows:

$$\mathbf{B}_{\perp n}(t) = B_0 \cos(2\pi f t)\tilde{\mathbf{u}} + B_0 \cos(2\pi f t)\tilde{\mathbf{v}} \tag{5}$$

where B_0 is the magnetic flux density at the center of the Helmholtz coils, f is the rotational frequency, and $(\tilde{\mathbf{u}},\tilde{\mathbf{v}})$ are the basis vectors of the plane orthogonal to the axis n. The Maxwell coil pair is capable of producing uniform field gradient parallel to the coaxis at the center. It consists of two identical coaxial circular coils with the same radius, but

are separated by $\sqrt{3}$ times the radius and the currents are in opposite direction. By appropriately setting the current flow in each coil, as shown in Fig. 1, a variety of magnetic fields can be created, such as rotating, oscillating, alternating, and conical magnetic fields. The electromagnets can be combined to generate very complex magnetic fields and allow multiple d.o.f. of motion for untethered magnetic robots. However, in these complex setups, the workspace is restricted compared to the volume of the whole system.

2) Permanent Magnets: Permanent magnets have the innate ability to generate strong and persistent magnetic fields. The strength and distribution of the magnetic field depend on the shape and size of the magnet. If the magnetic field $\mathbf{B}(\mathbf{p})$ is generated using a single actuator magnet, then its field at the magneic robot's position $\mathbf{p} \in \mathbb{R}^3$ relative to the actuator-magnet center, can be approximated by the point-dipole model such that,

$$\mathbf{B}(\mathbf{p}) = \frac{\mu_0}{4\pi\|\mathbf{p}\|^3}\left(3\hat{\mathbf{p}}\hat{\mathbf{p}}^{\mathsf{T}} - \mathbb{I}\right)\mathbf{M} = \frac{\mu_0}{4\pi\|\mathbf{p}\|^3}\mathbf{H}\mathbf{M}, \qquad (6)$$

where $\mu_0 = 4\pi \times 10^{-7}$ N·A^{-2} is the permeability of free space, $\mathbf{M} \in \mathbb{R}^3$ is the dipole moment of the actuator magnet, $\mathbb{I} \in \mathbb{R}^{3\times3}$ is the identity matrix [1] and $\mathbf{H} = 3\hat{\mathbf{p}}\hat{\mathbf{p}}^{\top} - \mathbb{I}$. Equation (6) exactly predicts the field produced by a spherical magnet. For all other geometries, it is an approximation that becomes more accurate with increasing distance.

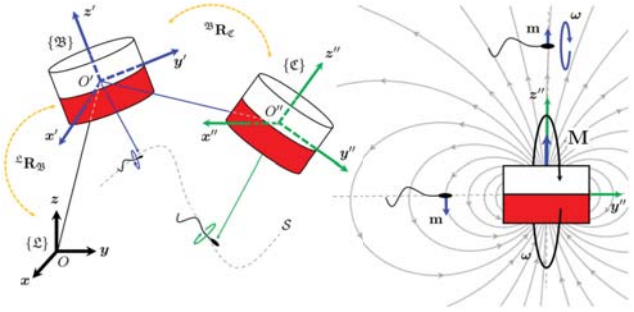

Fig. 2: Permanent magnets with axial or radial magnetization are translated, oriented, and rotated to simultaneously direct and actuate small scale untethered magnetic robots. Permanent magnet-based manipulation systems rely on the position and orientation of the actuating permanent magnet as the control inputs. Therefore, we consider rigid-body transformations of the actuating permanent magnet. A permanent magnet with axial magnetic moment $\mathbf{M}$ undergoes rigid-body displacement in a reference frame $\{\mathfrak{L}\}$. $\{\mathfrak{B}\}$ is the frame of reference of the magnet such that its orthonormal vector $\mathbf{z}'$ coincides with $\mathbf{M}$ and rotates about $\mathbf{y}'$ [32].

A non spherical geometry can be chosen to be well approximated by Equation (6) at smaller distances [2]. Since, the magnetic field produced is nonuniform and decreases with the distance, the exerted force $\mathbf{f}$ on the robot derived from (4) and (6) can be calculated by

$$\mathbf{f} = \frac{3\mu_0}{4\pi\|\mathbf{p}\|^4}\left(\hat{\mathbf{p}}\mathbf{m}^{\top} + \mathbf{m}\hat{\mathbf{p}}^{\top} + (\mathbf{m}^{\top}\hat{\mathbf{p}})\mathrm{Z}\right)\mathbf{M} = \mathbb{F}\mathbf{M} \qquad (7)$$

where the matrix $\mathrm{Z} = \mathrm{I} - 5\hat{\mathbf{p}}\hat{\mathbf{p}}^{\top}$. (6) conveys the fact that two parameters $\mathbf{p}$ and $\mathbf{M}$ (constant $\|\mathbf{M}\|$) influences the magnetic field at the region of interest; hence, the required magnetic field can be obtained by adjusting the position and/or orientation of the permanent magnet, as shown in Fig. 2. Therefore, permanent magnets are commonly associated with translational and/or rotational mechanisms. As the effects of translation and rotation on the magnetic field and field gradient are nonlinear, control of these systems are often achieved through nonlinear solution methods [15]. Equation (7) reveals the that the field gradient decreases faster with distance than the field intensity. Actuation with permanent magnets is significantly more complex due to non uniformity of the generated magnetic fields.

III. CONTROLLING ROTATING UNTETHERED MAGNETIC ROBOTS WITH A SINGLE ROTATING PERMANENT MAGNET (RPM)

A rotating permanent magnet generates a periodic magnetic field at a distance $\mathbf{p}$ from its center, which can be expressed from (6) as:

$$\mathbf{B}(\mathbf{p}, \mathrm{t} + 2\pi\mathrm{f}) = \mathbf{B}(\mathbf{p}, \mathrm{t}), \qquad (8)$$

where t is time and f is the rotational frequency. If a magnetic field given by $\mathbf{B}$ (8) is applied on an untethered magnetic robot with a dipole moment $\mathbf{m}$, then a magnetic torque $\boldsymbol{\tau}$ based on Equation (3) and a magnetic force $\mathbf{f}$ due to Equation (4) will be produced. The magnetic torque causes $\mathbf{m}$ to rotate in the direction of $\mathbf{B}$. If the magnetic field $\mathbf{B}$ rotates around an axis $\hat{\boldsymbol{\omega}}_{\mathrm{f}}$ (with direction of rotation given by the "right-hand" rule), then will cause $\mathbf{m}$ (and thus the robot) to continuously rotate. The magnetic force $\mathbf{f}$ causes the robot to translate in a direction determined by the robot's dipole moment $\mathbf{m}$ and the spatial derivative of the magnetic field. The untethered magnetic robot's propulsion can be produced using the magnetic torque to generate rotation, which is converted into propulsion via rolling or with a screw thread, the magnetic force can be employed for pulling, or both can be used in concert.

A. Rotation Axis of the Magnetic Field

For untethered robots that employ magnetic torque generated by the rotating magnetic field $\mathbf{B}$ for propulsion, appropriately selecting the rotation axis $\hat{\boldsymbol{\omega}}_{\mathrm{f}}$ of the magnetic field is a critical component of the control strategy. For robots in free medium (e.g., helical microswimmers in fluid) or those that roll, the robot's rotation axis naturally aligns itself with $\hat{\boldsymbol{\omega}}_{\mathrm{f}}$ and varying $\hat{\boldsymbol{\omega}}_{\mathrm{f}}$ steers the robot. For screw-like robots constrained in a lumen (e.g., a magnetic capsule endoscope in the small intestine), $\hat{\boldsymbol{\omega}}_{\mathrm{f}}$ should be locally aligned with the lumen in order to apply the most useful magnetic torque. The two most common methods to steer a robot is through axial control and radial control. During axial steering the RPM's axis $\hat{\boldsymbol{\Omega}}_{\mathrm{act}}$ of rotation moves on a sphere enclosing the untethered robot, such that the $\hat{\boldsymbol{\Omega}}_{\mathrm{act}}$ always points at the untethered robot. Any position on the $\hat{\boldsymbol{\Omega}}_{\mathrm{act}}$ axis is denoted to be in an axial position. During radial control

steering, the RPM moves on a circle in the plane defined by the untethered robot and the RPM's rotation axis $\hat{\mathbf{\Omega}}_{\text{act}}$ for 1 DOF, and it rotates about the radial line for the other DOF. In other words, any position in the plane spanned by the rotating $\mathbf{m}$ is a radial position. In these two positions, the rotating magnetic field $\mathbf{B}$ applied to the untethered robot rotates around an axis $\hat{\boldsymbol{\omega}}_{\text{f}}$ that lies parallel to the actuator magnet's rotation axis $\hat{\mathbf{\Omega}}_{\text{act}}$. Reversing the robot's direction is accomplished simply by changing the rotation direction of the RPM. Small steering inputs will result in the robot continually servoing to the desired steady state orientation. Moving the RPM manipulator closer/farther from the robot results in a change in the magnitude of the applied field and field gradient at the robot, but does not result in any steering.

Requiring the untethered robot to be exclusively operated in these two positions, however, significantly constrains the physical placement of the actuator magnet. To overcome this issue Mahoney et al [24] begin by reformulating this phenomenon in a manner that readily enables the solution of the inverse problem: finding the necessary RPM rotation axis $\hat{\mathbf{\Omega}}_{\text{act}}$ given a desired applied field rotation axis $\hat{\boldsymbol{\omega}}_{\text{f}}$, for any RPM position relative to the robot. The results enable a rotating magnetic field to be produced around an arbitrary axis $\hat{\boldsymbol{\omega}}_{\text{f}}$ in space using a single RPM in any position. Therefore, given $\hat{\boldsymbol{\omega}}_{\text{f}}$ and the untethered robot's position $\mathbf{p}$, the necessary actuator-magnet rotation axis $\hat{\mathbf{\Omega}}_{\text{act}}$ can be found with

$$\hat{\mathbf{\Omega}}_{\text{act}} = \widehat{\mathbf{H}\hat{\boldsymbol{\omega}}_{\text{f}}}. \tag{9}$$

The forward problem, which gives the local field axis of rotation $\hat{\boldsymbol{\omega}}_{\text{f}}$ at the position $\mathbf{p}$, given the actuator magnet's axis of rotation $\hat{\mathbf{\Omega}}_{\text{act}}$, is found with

$$\hat{\boldsymbol{\omega}}_{\text{f}} = \widehat{\mathbf{H}^{-1}\hat{\mathbf{\Omega}}_{\text{act}}} \tag{10}$$

where $\mathbf{H^{-1}} = (\mathbf{H} - \mathbb{I})/2$. The relation between the actuating magnet and untethered robot's rotation axis is given by Equations (8) and (9). This control strategy allows steering of untethered magnetic robots by controlling the rotation axis of the actuator magnet $\hat{\mathbf{\Omega}}_{\text{act}}$. The periodicity of the magnetic field generated by an RPM, as expressed in Equations (6), in combination with Equation (8) are used to define a closed-form relation between the rotational velocity of the field $\boldsymbol{\omega}_{\text{f}}$ and the RPM $\mathbf{\Omega}_{\text{act}} = 2\pi\text{f}$ rad/s. The relation depends on the maximum and minimum values of the field as follows:

$$\|\boldsymbol{\omega}_{\text{f}}(\text{t})\| = \left(\frac{\|\mathbf{B}\|_{\text{min}}\|\mathbf{B}\|_{\text{max}}}{\|\mathbf{B}(\text{t})\|^2}\right)\|\mathbf{\Omega}_{\text{act}}(\text{t})]\|. \tag{11}$$

REFERENCES

[1] Peyer, Kathrin E., Li Zhang, and Bradley J. Nelson. "Bio-inspired magnetic swimming microrobots for biomedical applications." Nanoscale 5.4 (2013): 1259-1272.

[2] Sitti, Metin. "Miniature soft robots—road to the clinic." Nature Reviews Materials 3.6 (2018): 74-75.

[3] Sitti, Metin, Hakan Ceylan, Wenqi Hu, Joshua Giltinan, Mehmet Turan, Sehyuk Yim, and Eric Diller. "Biomedical applications of untethered mobile milli/microrobots." Proceedings of the IEEE 103, no. 2 (2015): 205-224.

[4] S. Yim, E. Gultepe, D. H. Gracias, and M. Sitti, "Biopsy using a magnetic capsule endoscope carrying, releasing, and retrieving untethered microgrippers," IEEE Transactions on Biomedical Engineering, vol. 61, no. 2, p. 513–521, 2014.

[5] C. K. Schmidt, M. Medina-S anchez, R. J. Edmondson, and O. G. Schmidt, "Engineering microrobots for targeted cancer therapies from a medical perspective," Nature Communications, vol. 11, no.1, 2020.

[6] O. Ergeneman, G. Chatzipirpiridis, J. Pokki, M. Marin-Su arez, G. A. Sotiriou, S. Medina-Rodriguez, J. F. F.Sanchez, A. Fernandez-Guti errez, S. Pane, B. J. Nelson, and et al., "In vitro oxygen sensing using intraocular microrobots," IEEE Transactions on Biomedical Engineering, vol. 59, no. 11, p. 3104–3109, 2012.

[7] B. J. Nelson, I. K. Kaliakatsos, and J. J. Abbott, "Microrobots for minimally invasive medicine," Annual Review of Biomedical Engineering, vol. 12, no. 1, p. 55–85, 2010.

[8] I. S. M. Khalil, A. F. Tabak, K. Sadek, D. Mahdy, N. Hamdi, and M. Sitti, "Rubbing against blood clots using helical robots: Modeling and in vitro experimental validation," IEEE Robotics and Automation Letters, vol. 2, no. 2, p. 927–934, 2017.

[9] Fischer, Peer, and Ambarish Ghosh. "Magnetically actuated propulsion at low Reynolds numbers: towards nanoscale control." Nanoscale 3, no. 2 (2011): 557-563.

[10] Xu, Tiantian, Jiangfan Yu, Xiaohui Yan, Hongsoo Choi, and Li Zhang. "Magnetic actuation based motion control for microrobots: An overview." Micromachines 6, no. 9 (2015): 1346-1364.

[11] Heunis, C. M., J. Sikorski, and S. Misra. "Magnetic actuation of flexible surgical instruments for endovascular interventions." IEEE robotics automation magazine (2017).

[12] Hwang, Junsun, Jin-young Kim, and Hongsoo Choi. "A review of magnetic actuation systems and magnetically actuated guidewire- and catheter-based microrobots for vascular interventions." Intelligent Service Robotics 13, no. 1 (2020): 1-14.

[13] I. S. M. Khalil, L. Abelmann, and S. Misra, "Magnetic-based motion control of paramagnetic microparticles with disturbance compensation," IEEE Transactions on Magnetics, vol. 50, no. 10, pp. 1–10, 2014.

[14] E. B. Steager, M.S. Sakar, C. Magee, M. Kennedy, A. Cowley, and V. Kumar, "Automated biomanipulation of single cells using magnetic microrobots," The International Journal of Robotics Research, vol. 32, no. 3, pp. 346–359, 2013.

[15] A. W. Mahoney, and J. J. Abbott, "Five-degree-of-freedom manipulation of an untethered magnetic device in fluid using a single permanent magnet with application in stomach capsule endoscopy," The International Journal of Robotics Research, vol. 35, pp.129–147, 2016.

[16] P. Valdastri, M. Simi, and R. J. Webster III, "Advanced technologies for gastrointestinal endoscopy," Annual Review of Biomedical Engineering, vol. 14, pp. 297–429, 2012.

[17] M. P. Kummer, J. J. Abbott, B. E. Kratochvil, R. Borer, A. Sengul, and B. J. Nelson, "Octomag: An electromagnetic system for 5-DOF wireless micromanipulation," IEEE Transactions on Robotics, vol. 26, no. 6, pp. 1006–1017, 2010.

[18] A. J. Petruska et al., "Magnetic Needle Guidance for Neurosurgery: Initial Design and Proof of Concept," IEEE Int. Conf. on Robotics and Automation, pp. 4392–4397, 2016.

[19] F. Carpi and C. Pappone, "Stereotaxis niobe magnetic navigation system for endocardial catheter ablation and gastrointestinal capsule endoscopy," Expert Review of Medical Devices, vol. 6, no. 5, pp. 487–498, 2009.

[20] F. P. Gosselin, V. Lalande, and S. Martel, "Characterization of the deflections of a catheter steered using a magnetic resonance imaging system," Medical Physics, vol.38, no. 9, pp. 4994–5002, 2011.

[21] Ko, Youngho, Sungyoung Na, Youngwoo Lee, Kyoungrae Cha, Seong Young Ko, Jongoh Park, and Sukho Park. "A jellyfish-like swimming mini-robot actuated by an electromagnetic actuation system." Smart Materials and Structures 21, no. 5 (2012): 057001.

[22] Gao, Wei, Sirilak Sattayasamitsathit, Kalayil Manian Manesh, Daniel Weihs, and Joseph Wang. "Magnetically powered flexible metal nanowire motors." Journal of the American Chemical Society 132, no. 41 (2010): 14403-14405.

[23] Frutiger, Dominic R., Karl Vollmers, Bradley E. Kratochvil, and Bradley J. Nelson. "Small, fast, and under control: wireless resonant magnetic micro-agents." The International Journal of Robotics Research 29, no. 5 (2010): 613-636.

[24] Huang, Tian-Yun, Famin Qiu, Hsi-Wen Tung, Xue-Bo Chen, Bradley J. Nelson, and Mahmut Selman Sakar. "Generating mobile fluidic traps for selective three-dimensional transport of microobjects." Applied Physics Letters 105, no. 11 (2014): 114102.

[25] K. B. Yesin, K. Vollmers, and B. J. Nelson, "Modeling and Control of Untethered Biomicrorobots in a Fluidic Environment Using Electromagnetic Fields," The International Journal of Robotics Research, vol. 25, pp. 527-536, 2006.

[26] Choi, Jongho, Hyunchul Choi, Kyoungrae Cha, Jong-oh Park, and Sukho Park. "Two-dimensional locomotive permanent magnet using electromagnetic actuation system with two pairs stationary coils." In 2009 IEEE International Conference on Robotics and Biomimetics (ROBIO), pp. 1166-1171. IEEE, 2009.

[27] Hu, Chengzhi, Carlos Tercero, Seiichi Ikeda, Toshio Fukuda, Fumihito Arai, and Makoto Negoro. "Modeling and design of magnetic sugar particles manipulation system for fabrication of vascular scaffold." In 2011 IEEE/RSJ International Conference on Intelligent Robots and Systems, pp. 439-444. IEEE, 2011.

[28] Fountain TWR, Kailat PV and Abbott JJ , "Wireless control of magnetic helical microrobots using a rotating-permanent magnet manipulator," IEEE international conference on robotics and automation (ICRA '10), pp. 576–581, 2010.

[29] AW Mahoney, DL Cowan, KM Miller, JJ Abbott,"Control of untethered magnetically actuated tools using a rotating permanent magnet in any position." IEEE International Conference on Robotics and Automation, 3375-3380, 2012.

[30] Avaneesh, R., Venezian, R., Kim, C.S., Park, J.O., Misra, S. and Khalil, I.S., 2021, October. Open-Loop Magnetic Actuation of Helical Robots using Position-Constrained Rotating Dipole Field. In 2021 IEEE/RSJ International Conference on Intelligent Robots and Systems (IROS) (pp. 8545-8550). IEEE.

[31] Venezian, R., Khalil, I. S. (2022). Understanding Robustness of Magnetically Driven Helical Propulsion in Viscous Fluids Using Sensitivity Analysis. Advanced Theory and Simulations, 5(4), 2100519.

[32] Khalil, I.S., Klingner, A. and Misra, S., 2021. Mathematical modeling of swimming soft microrobots. Academic Press.

Chapter 2: Open-Loop Magnetic Actuation of Helical Robots using Position-Constrained Rotating Dipole Field

Abstract— **Control of tetherless magnetically actuated helical robots using rotating dipole fields has a wide variety of medical applications. The most promising technique in manipulation of these robots involves a rotating permanent magnet controlled by a robotic manipulator. In this work, we study the open-loop response of helical robots (in viscous fluids characterized by low Reynolds numbers) in the presence of position constraints on the actuating rotating permanent magnet. We first derive a mapping between the space of the manipulator's joints, the produced magnetic fields in three-dimensional space, and the translational and rotational velocities of the helical robot. Then, we constrain the 3D position of the rotating dipole field and predict the response of the helical robot by controlling its angular velocity using the constrained mapping. We demonstrate open-loop control and gravity compensation of the robot using the angular velocities of the actuating permanent magnet while enforcing constraints on the end-effector position.**

I. INTRODUCTION

Over the past decade, robots at the nano- and micro-scales have shown potential to revolutionize medicine by reaching regions inaccessible to catheterization [1]–[4]. The locomotion of these tetherless devices capitalizes on the conversion of several forms of energies into mechanical energy or movement. Magnetic [5], [6], acoustic [7], chemical [8], electric [9], thermal [10], and light [11] energy have been utilized to actuate structures fabricated specifically to work upon sensing one, or a combination [12], of these external stimuli. Once the relation between the external energy and the behavior of the stimuli-responsive material in the fabricated structures is understood, a locomotion strategy is designed to work based on the environment and the potential application. For example, rolling or tumbling on a solid boundary [13], [14], swimming using the drag-based thrust [15], and pulling with a force [16] have been proven to be efficient locomotion strategies. The form of energy and the locomotion strategy must be selected specifically based on the physical surroundings, intended application, and the localization strategy. In practice, magnetic actuation using the drag-based thrust of helical microrobots is efficient under a wide range of Reynolds numbers (*Re*). In this case, it is reasonable to power these microrobots using actuating time-varying magnetic field produced by rotating permanent magnets fixed to the end-effector of a manipulator [17], as shown in Fig. 1. Scalability and adaptability are two direct consequences of the fact that the displacement of the actuating permanent magnet can be fully controlled in three-dimensional (3-D) space. First, the size of the workspace is no longer limited by the projection distance of the magnetic field, but rather depends on the relatively large workspace of the manipulator. Second, the configuration of

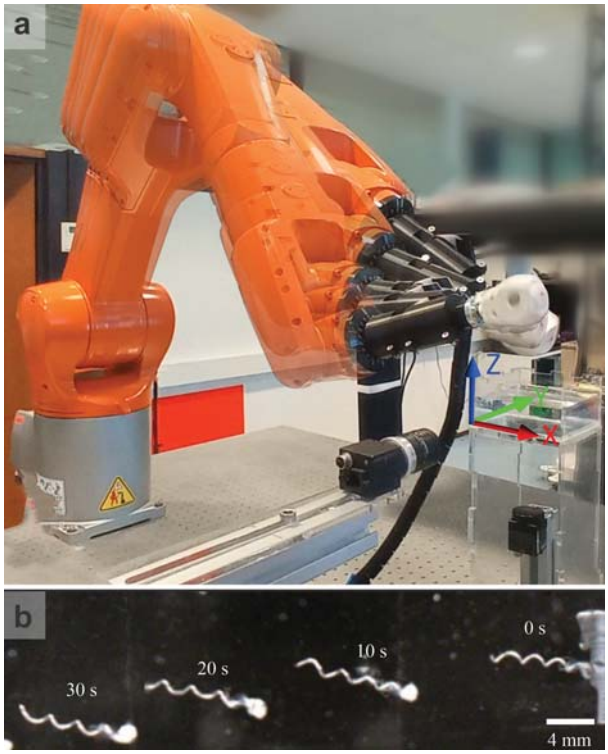

Fig. 1: Helical propulsion in viscous fluid is achieved using rotating magnetic fields. (a) An actuating rotating permanent magnet is controlled in three-dimensional (3-D) space by a six degree-of-freedom robotic manipulator. (b) The produced time-varying magnetic field drives a helical robot controllably inside a viscous fluid. The helical robot is controlled while enforcing a position constraint on actuating dipole field.

this permanent magnet-based robotic system can be adapted to incorporate important functionalities like non-invasive imaging systems [18].

It has been shown that when a magnetic dipole, is rotated around a fixed axis such that the dipole is perpendicular to the axis of rotation, the magnetic field vector at every point in space also rotates around a fixed axis [17]. Mahoney *et al.* have reformulated this phenomenon using linear algebraic techniques, which enables finding the necessary dipole rotation axis that is required to make the magnetic field at any desired point in space rotate about any desired axis [17]. Such method has been tested using a rotating permanent magnet fixed in space by a robotic manipulator to control the displacement of the magnet, and actuation of capsule endoscopes, helical swimmers, and spherical agents have been demonstrated inside fluid-filled confined environments. They have also demonstrated closed-loop control of three degree-

of-freedom (3-DOF) and 2-DOF open-loop directional control of a magnetic capsule endoscope based on position feedback only [19]. These control results are implemented in the absence of constraints on the displacement of the actuating dipole field or the robotic manipulator.

In this paper, we control the motion of helical robots inside a viscous fluid in 3-D space using a rotating magnetic field produced by an actuating permanent magnet fixed to a robotic manipulator. We demonstrate the ability of the system to control the motion of the helical robot in the presence of a position constraint on the end-effector. We focus on changing the actuation axis of the rotating dipole field while keeping the magnet position fixed over time to follow a prescribed path whilst compensating for gravity in an open-loop way.

II. Modeling of Helical Propulsion and Magnetic Actuation

In low-Re, the response of the robot to an externally applied magnetic field is governed by balance between magnetic, viscous drag, and gravitational forces and torques.

A. Helical Propulsion in Low-Re

Suppose we consider a helical body with length L and magnetic moment $\mathbf{m}$ perpendicular to its helix axis, immersed in a viscous fluid, with density ρ_{f}, characterized by low-Re and actuated using non-uniform magnetic field, $\mathbf{B}$, as shown in Fig. 2. In low-Re, inertial forces are negligible and the motion of helical robot is governed by

$$\mathbf{f}_{\mathrm{visc}} + \mathbf{f}_{\mathrm{mag}} + \mathbf{f}_{\mathrm{g}} = 0 \quad (1)$$

$$\mathbf{T}_{\mathrm{visc}} + \mathbf{T}_{\mathrm{mag}} + \mathbf{T}_{\mathrm{g}} = 0, \quad (2)$$

where $\mathbf{f}_{\mathrm{visc}}$ and $\mathbf{T}_{\mathrm{visc}}$ are the viscous drag force and torque, respectively. Further, $\mathbf{f}_{\mathrm{mag}}$ and $\mathbf{T}_{\mathrm{mag}}$ are the magnetic force and torque, respectively. Furthermore, $\mathbf{f}_{\mathrm{g}}$ and $\mathbf{T}_{\mathrm{g}}$ are the force and torque due to gravity, respectively. One direct consequence of the negligible inertia force is that the hydrodynamics is linear. Therefore, the viscous drag force and torque are given by

$$\begin{pmatrix} \mathbf{f}_{\mathrm{visc}} \\ \mathbf{T}_{\mathrm{visc}} \end{pmatrix} = \begin{pmatrix} \boldsymbol{A} & \boldsymbol{B} \\ \boldsymbol{B}^{\mathrm{T}} & \boldsymbol{C} \end{pmatrix} \begin{pmatrix} \mathbf{U} \\ \boldsymbol{\omega} \end{pmatrix}, \quad (3)$$

where $\mathbf{U}$ and $\boldsymbol{\omega}$ are the translational and angular velocity of the helical body due to the external force and torque, respectively. In Equation (3) the sub-matrices $\boldsymbol{A}$, $\boldsymbol{B}$, and $\boldsymbol{C}$ are calculated using the Resistive-Force Theory and are only dependent on the viscosity, η, of the medium and the geometry of the helical body [15]. In Equations (1)-(2), the magnetic force, $\mathbf{f}_{\mathrm{mag}}(\boldsymbol{p})$, and torque, $\mathbf{T}_{\mathrm{mag}}(\boldsymbol{p})$ at point, $\boldsymbol{p}$, are given by

$$\mathbf{f}_{\mathrm{mag}}(\boldsymbol{p}) = (\mathbf{m} \cdot \nabla)\mathbf{B}(\boldsymbol{p}) \quad (4)$$

$$\mathbf{T}_{\mathrm{mag}}(\boldsymbol{p}) = \mathbf{m} \times \mathbf{B}(\boldsymbol{p}). \quad (5)$$

Finally, in Equations (1)-(2) the force, $\mathbf{f}_{\mathrm{g}}$, and torque, $\mathbf{T}_{\mathrm{g}}$, exerted on the helical robot due to gravity are given by

$$\mathbf{f}_{\mathrm{g}} = V(\rho_{\mathrm{r}} - \rho_{\mathrm{f}})\mathbf{g} \quad (6)$$

$$\mathbf{T}_{\mathrm{g}} = (\mathbf{r}_{\mathrm{cov}} - \mathbf{r}_{\mathrm{com}}) \times \mathbf{f}_{\mathrm{g}}, \quad (7)$$

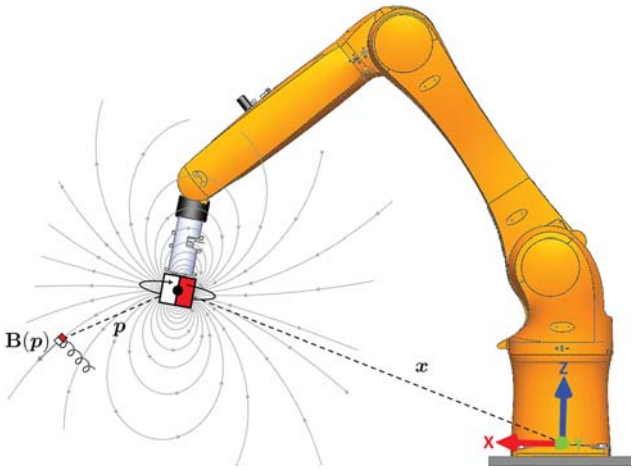

Fig. 2: A rotating actuating magnetic field, $\mathbf{B}(\boldsymbol{p})$, is produced by a permanent magnet. The displacement of the permanent magnet is controlled by a robotic manipulator. A helical robot with magnetic moment perpendicular to its long axis aligns along the rotating field lines and achieve helical propulsion in viscous fluid.

where V is the volume the robot, ρ_{r} and ρ_{f} are its density and the density of the fluid, respectively. Furthermore, $\mathbf{g}$ signifies gravity, $\mathbf{r}_{\mathrm{cov}}$ and $\mathbf{r}_{\mathrm{com}}$ are the position vectors of the center of volume and center of mass, respectively. These force and torque complete the relation between the external forces and torques and the resulting velocities $\mathbf{U}$ and $\boldsymbol{\omega}$ of the robot.

B. Rotating Actuating Magnetic Fields

Equations (1)-(3) show the velocities of the helical robots can be directly determined from the balance between magnetic force, force due to gravity, and viscous drag. The magnetic force and torque are directly affected by the actuating magnetic field, $\mathbf{B}(\boldsymbol{p})$, which is given by the following point-dipole approximation:

$$\mathbf{B}(\boldsymbol{p}) = \frac{\mu_0}{4\pi}\left(\frac{3\boldsymbol{p}\boldsymbol{p}^{\mathrm{T}}}{\|\boldsymbol{p}\|^5} - \frac{\mathbb{I}}{\|\boldsymbol{p}\|^3}\right)\mathbf{M}(\boldsymbol{q}), \quad (8)$$

where $\mu_0 = 4\pi \times 10^{-7}$ N.A^{-2} is the permeability of free space, $\mathbf{M} \in SO(3)$ is the dipole moment of the actuator magnet and $\mathbb{I} \in \mathbb{R}^{3\times3}$ is the identity matrix. Equation (8) gives the magnetic field at the position of the robot, $\boldsymbol{p}$, when the permanent magnet is fixed at $\boldsymbol{x} \in \mathbb{R}^3$. Note that the magnetic field at a point, $\boldsymbol{p}$, is controlled by the joints of the manipulator.

The configuration-to-pose kinematics of the robotics manipulator is given by [20]

$$\{\boldsymbol{x}, R\} = \mathcal{F}(\boldsymbol{q}), \quad (9)$$

where $\mathcal{F} : \mathbb{R}^n \rightarrow \{\mathbb{R}^3, SO(3)\}$ is the forward kinematic mapping and $\boldsymbol{q} \in \mathbb{R}^n$ is the joint variables. Equations (8) and (9) provide the relation between the magnetic field at a point, $\boldsymbol{p}$, and the configuration of the robotic manipulator. Fig. 3 shows the magnetic field at a point calculated using Equation (8) and the corresponding position and orientation of the end-effector for a time-varying joint variables. It is

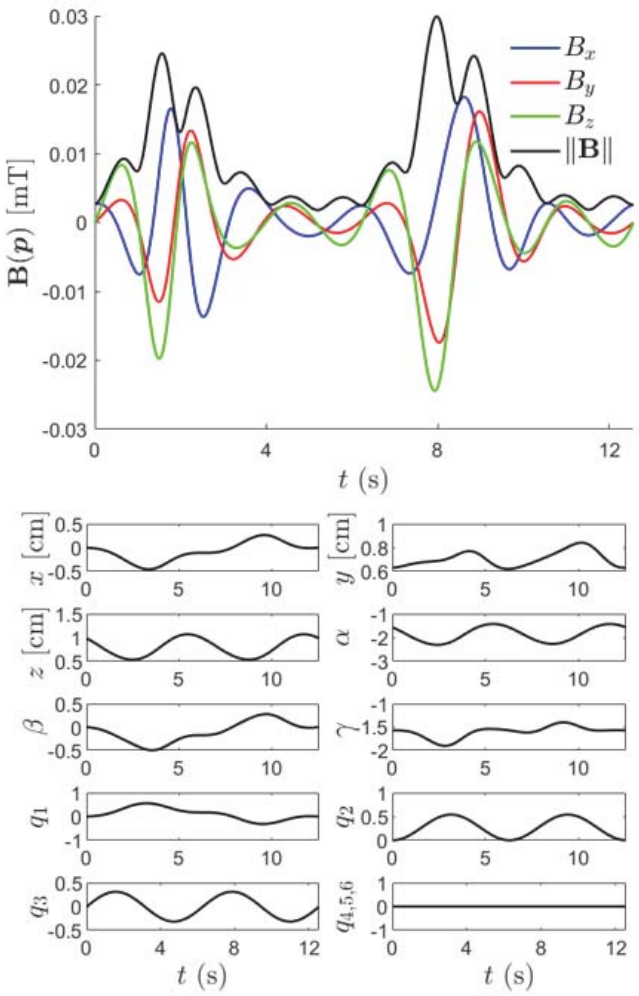

Fig. 3: The magnetic field at a point, $\boldsymbol{p}$, from the actuator magnet varies with the joint variables of the robotic manipulator $(q_1, \ldots, q_6)$. The coordinates x, y, and z characterize the position of the actuator magnet in the manipulator frame of reference, and the angles α, β, and γ characterize the orientation R.

convenient to represent the composed linear and angular velocities of the end-effector by the joint velocity, we have

$$\begin{pmatrix} \dot{\boldsymbol{x}} \\ \boldsymbol{\Omega} \end{pmatrix} = \mathbf{J}_{\mathrm{m}}(\boldsymbol{q})\dot{\boldsymbol{q}}, \tag{10}$$

where $\mathbf{J}_{\mathrm{m}} \in \mathbb{R}^{n\times n}$ is the manipulator Jacobian.

Mahoney and Abbott have shown that the velocity level kinematics (10) can also be modified to include the contribution of the magnetic moment of the actuator magnet using $\dot{\mathbf{M}} = \Omega \times \mathbf{M}$, and we obtain [19]

$$\begin{pmatrix} \dot{\boldsymbol{x}} \\ \dot{\mathbf{M}} \end{pmatrix} = \begin{pmatrix} \mathbb{I} & 0 \\ 0 & \mathrm{SK}(\mathbf{M}) \end{pmatrix} \mathbf{J}_{\mathrm{m}}(\boldsymbol{q})\dot{\boldsymbol{q}} = \mathbf{J}_{\mathrm{A}}(\boldsymbol{q})\dot{\boldsymbol{q}}, \tag{11}$$

where $\mathrm{SK}(\cdot) : \mathbb{R}^3 \to SO(3)$ is the skew-symmetric operator of the cross product and $\mathbf{J}_{\mathrm{A}} \in \mathbb{R}^{n\times n}$ is the actuator permanent magnet Jacobian. Equation (11) completes the relation between the joint velocities of the manipulator and the helical robot velocity, composed by the linear velocity $\mathbf{U}$ and the angular velocity $\boldsymbol{\omega}$.

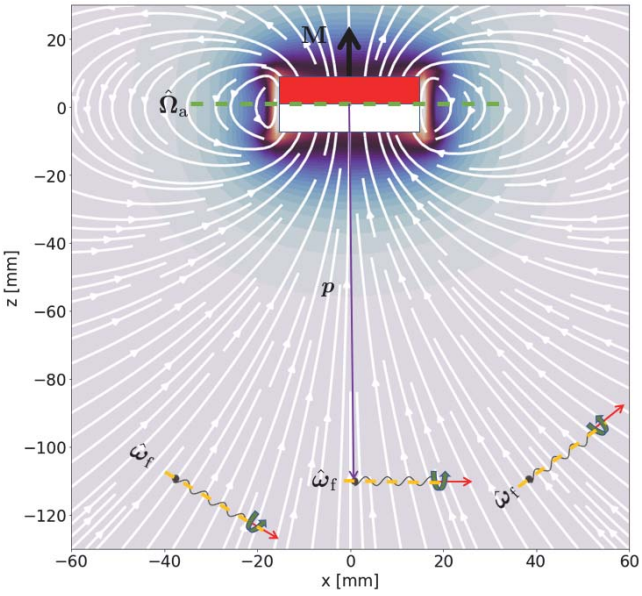

Fig. 4: Magnetic field lines generated by a permanent magnet with magnetization $\mathbf{M} = 18.89$ A.m^2 and $\|\mathbf{B}(\boldsymbol{p})\| = 2.75$ mT at $\boldsymbol{p} = \begin{bmatrix} 0 & 0 & -110 \end{bmatrix}^{\mathrm{T}}$ mm. The magnetic dipole moment of the helical robot is aligned along the magnetic field rotation axis, $\hat{\boldsymbol{\omega}}_{\mathrm{f}}$. Control of the axis of rotation of the actuator magnet, $\hat{\boldsymbol{\Omega}}_{\mathrm{a}}$, enables the robot to swim controllably and compensate its own weight.

C. Actuation using Pose-Constrained Dipole Field

To test the helical propulsion under a position constraint on the actuator magnet, we shall invoke $\dot{\boldsymbol{x}} = 0$ into Equation (12), which yields

$$\begin{pmatrix} 0 \\ \dot{\mathbf{M}} \end{pmatrix} = \begin{pmatrix} \mathbf{J}_{\mathrm{m}}^{11}(\boldsymbol{q}) & \mathbf{J}_{\mathrm{m}}^{12}(\boldsymbol{q}) \\ \mathrm{SK}(\mathbf{M})\mathbf{J}_{\mathrm{m}}^{21}(\boldsymbol{q}) & \mathrm{SK}(\mathbf{M})\mathbf{J}_{\mathrm{m}}^{22}(\boldsymbol{q}) \end{pmatrix} \dot{\boldsymbol{q}}, \tag{12}$$

where $\mathbf{J}_{\mathrm{m}}^{11}(\boldsymbol{q})$, $\mathbf{J}_{\mathrm{m}}^{12}(\boldsymbol{q})$, $\mathbf{J}_{\mathrm{m}}^{21}(\boldsymbol{q})$, and $\mathbf{J}_{\mathrm{m}}^{22}(\boldsymbol{q})$ are the submatrices of the geometric Jacobian. Equations (12) maps the joint velocities into angular velocity of the actuator magnet without translation. If the translation and rotation of the actuator magnet are kept constant (Fig. 4), then the helical robot will ultimately align along the the magnetic field $\mathbf{B}(\boldsymbol{p})$. In this case, the magnetic field rotation axis, $\hat{\boldsymbol{\omega}}_{\mathrm{f}}$, and the actuator magnet's rotation axis, $\hat{\boldsymbol{\Omega}}_{\mathrm{a}}$, are given as $\hat{\boldsymbol{\Omega}}_{\mathrm{a}} = \widehat{\mathbf{H}\hat{\boldsymbol{\omega}}_{\mathrm{f}}}$, where $\mathbf{H} = 3\hat{\boldsymbol{p}}\hat{\boldsymbol{p}}^{\mathrm{T}} - \mathbb{I}$. Therefore, the rotation axis of the magnetic field varies with the position of the helical robot with respect to the actuator magnet, $\boldsymbol{p}$, and it is not possible to maintain the swimming direction along a straight line (along the $\mathbf{x}$-axis). The angular velocity of the actuator magnet must be controlled using Equation (12) to orient the rotation axis of the magnetic field parallel to the $\mathbf{x}$-axis and enable forward swimming.

III. Experimental Results

Open-loop motion control experiments are conducted using the permanent magnet-based robotic system shown in Fig. 1 to drive the robot along a prescribed path while enforcing a constraint on the end-effector, as shown in Fig. 5.

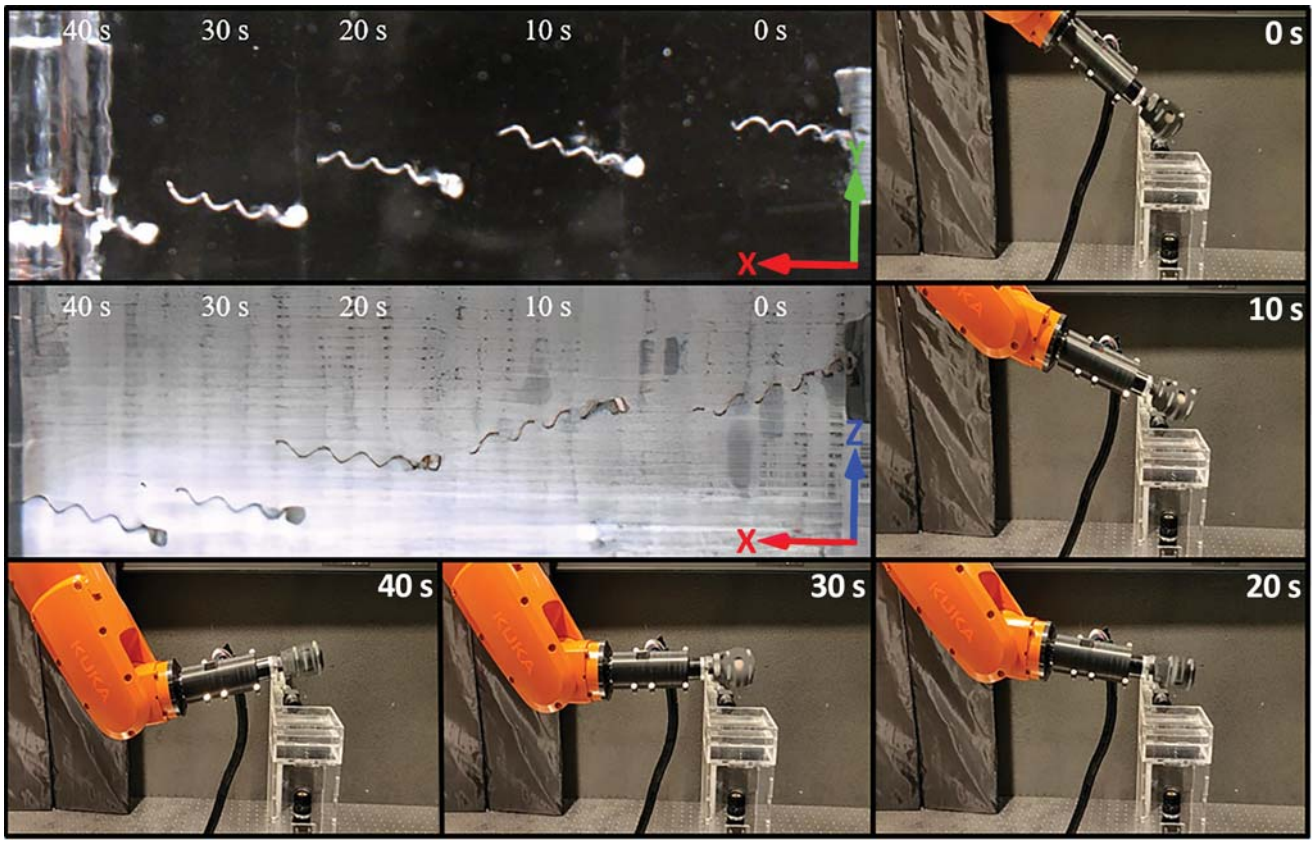

Fig. 5: Motion control achieves helical propulsion in the presence of a constraint on the position of the actuating permanent magnet. The robot swims controllably under the influence of a rotating magnetic field at actuation frequency of 5 Hz. The robot swims at a maximum velocity of $U = 1.43$ mm/s in silicon oil with density $\rho_{\mathrm{f}} = 971$ kg/m^3 and viscosity of $\eta = 1$ Pa.s ($Re = 10^{-2}$).

A. System Description

Our system consists of a 6-DOF serial manipulator (KUKA KR-1100-2, KUKA, Augsburg, Germany) to control the displacement of the rotating disc permanent magnet. The magnet (NdFeB Grade-N45) has a diameter of 35 mm, height of 20 mm, and is axially magnetized. The magnetic flux density of the actuator magnet is measured using a SENIS 3-axis digital Teslameter at varying distance, $\boldsymbol{p}$. The magnitude of the dipole moment $\|\mathbf{M}\|$ is determined using a least squares solution for the point-dipole model. In this experiment, 50 samples of the flux density are measured between 40 mm and 100 mm from the center of the magnet, resulting in $\|\mathbf{M}\| = 18.89$ A.m^2.

The disc magnet is actuated by a Maxon 18V brushless DC motor with Hall-effect sensors, encoder and a planetary gearbox with gear ratio of 3.7:1. The motor is controlled using an EPOS4 Compact 50/5 CAN, digital position controller. The continuous rotation of the permanent magnet enables the robot to achieve helical propulsion. The kinematics and the Denavit-Hartenberg parameters from the base frame to the end-effector and to the actuator magnet frames of reference are provided in Appendix A.

The robot consists of a cylindrical permanent magnet (NdFeB Grade-N52) with diameter of 1 mm and height of 1 mm, attached to a helical body such that the helix axis is perpendicular to the dipole moment. The helix has length, pitch and radius of 11.7 mm, 3 mm and 0.6 mm, respectively. The robot is immersed in silicon oil (reservoir of dimensions 100 mm $\times$ 100 mm $\times$ 50 mm) with density of $\rho_{\mathrm{f}} = 970$ kg/m^3 and viscosity of $\eta = 1$ Pa.s. Motion of the robot is measured using two FLIR Blackfly cameras in the $\mathbf{x}$-$\mathbf{y}$ and $\mathbf{x}$-$\mathbf{z}$ plane. Both cameras are fitted with Fujinon lens of 6 mm fixed focal length producing sub-millimeter tracking accuracy at 60 frames per second.

The entire system is programmed and modeled through Matlab Interface (Version R2020a). To achieve real-time control of the the robotic manipulator, a connection between RoboDK (RoboDK Inc., Montreal, Canada) and the robotic manipulator was established to move it automatically using RoboDK's user interface. The connection was established through a standard Ethernet connection (TCP/IP). For this purpose, a KUKAVARPROXY (Imts Srl, Taranto, Italy) server was installed on the KRC4 controller (KUKA, Augsburg, Germany) of the robotic manipulator. This server allows the global variables from the robotic arm controller to be exchanged with the remote RoboDK's user interface.

B. Open-Loop Control of the Helical Robot

To control the helical robot along a desired path it is critical to select the appropriate rotation axis $\hat{\boldsymbol{\omega}}_{\mathrm{f}}$ of the magnetic field. When the robot swims away from the nearby solid boundary and in the absence of any interactions, its rotation axis aligns with $\hat{\boldsymbol{\omega}}_{\mathrm{f}}$. Therefore, it is convenient to

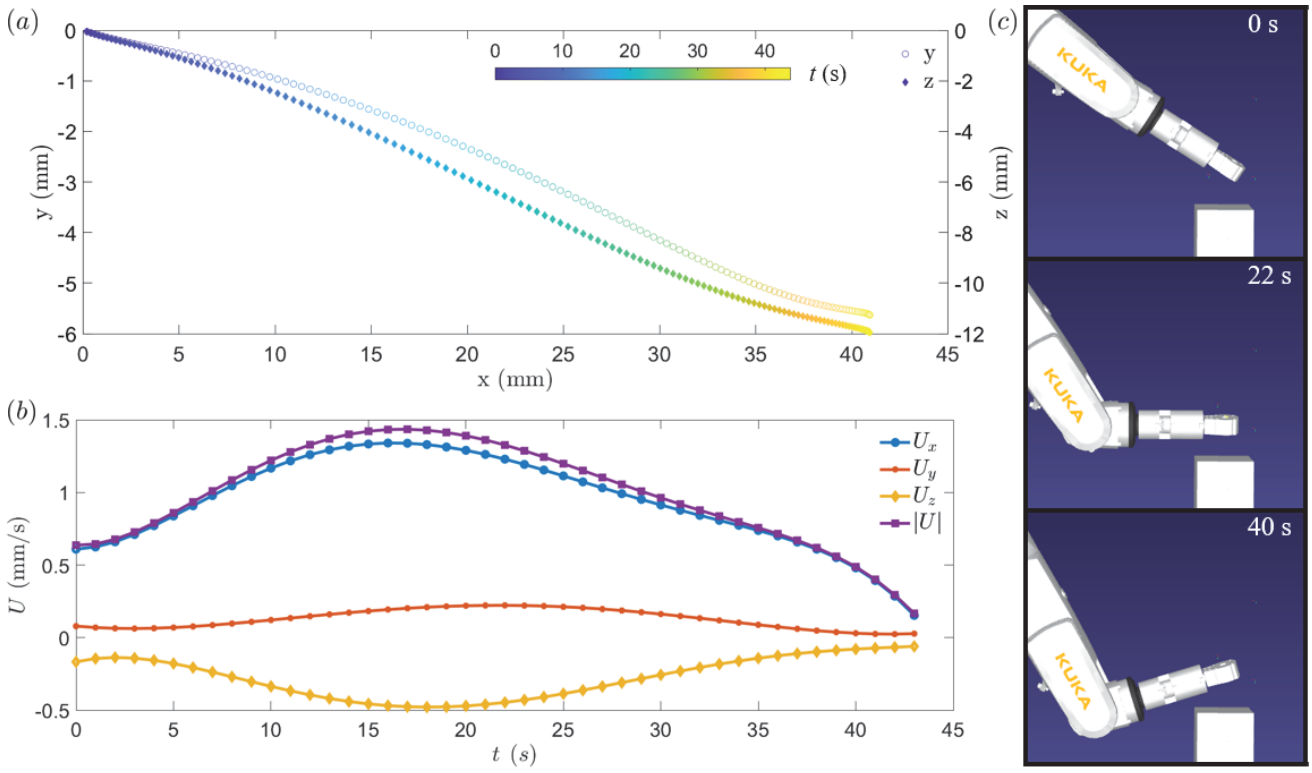

Fig. 6: Experimental motion control result demonstrates swimming under the influence of a rotating field produced by a constrained actuating magnet. The robot swims in silicone oil ($\rho_{\mathrm{f}} = 971$ kg/m^3 and $\eta = 1$ Pa.s) at an average speed of $U = 0.98$ mm/s and has Reynolds number of $Re = 10^{-3}$. Maximum swimming speed is achieved at $t = 17$ seconds when the robot swims toward the permanent magnet and the magnetic force contributes to its propulsive thrust.

steer the helical robot by controlling $\hat{\boldsymbol{\Omega}}_{\mathrm{a}}$. In addition, the rotation axis of the magnetic actuator can be determined using the prescribed trajectory of the desired path such that $\hat{\boldsymbol{\omega}}_{\mathrm{f}}$ and the local tangent are perpendicular.

Fig. 5 shows a representative open-loop control result of the helical robot along a straight line along the $\mathbf{x}$-axis. Therefore, the rotation axis of the magnetic field, $\hat{\boldsymbol{\omega}}_{\mathrm{f}}$, is made parallel to the $\mathbf{x}$-axis, while the constraint on the position of the actuating permanent magnet is enforced using Equations (12). In this experiment, the robot swims at a maximum swimming speed of $U = 1.43$ mm/s at actuation frequency of 5 Hz. The step-out frequency of the robot is 12 Hz. Therefore, the swimming speed of the robot can be controlled by increasing the actuation frequency of the magnetic field below the step-out frequency. In this case, the angular velocity of the rotating dipole field will depend on the linear velocity of the robot based on Equations (1)-(8).

The swimming path of the helical robot is shown in the $\mathbf{x}$-$\mathbf{y}$ and $\mathbf{x}$-$\mathbf{z}$ planes. This experimental result shows that associated with the translational motion of the helical robot is a continuous change in the angular velocity of the actuator magnet, as shown using the representative configurations of the robotic manipulator at $t = 0$, $t = 22$, and $t = 40$ seconds. The helical robot swims at an average velocity of 0.98 mm/s along the $\mathbf{x}$-axis and 0.15 mm/s along the $\mathbf{y}$-axis, as shown in Fig. 6. The average speed of the robot along the $\mathbf{z}$-axis is 0.3 mm/s. For $0 < t \leq 20$ seconds, the forward swimming speed of the robots increases as the distance to the actuator magnet decreases. At $t > 20$ seconds, the swimming speed decreases at the same rate as the gap with the actuator magnet increases. The positive and negative slopes of the forward swimming velocity signifies that the magnetic force (4) plays an important role and contributes to the net propulsive thrust of the robot. At $t = 22$ seconds, the robot is radially-actuated as the axis of the actuating magnet and the long axis of the robot are aligned. As the robot moves away from the actuator magnet, the magnetic force acts against the propulsive trust and we observe a noticeable decrease in the swimming speed, as shown in Fig. 6.

IV. Conclusions and Future Work

Magnetic actuation of helical robots is achieved using a rotating dipole field in the presence of a constraint on its position. We derive the mapping between the robot velocity, composed by linear and angular velocity, and the joint velocities of the robotic manipulator which fix the constrained rotating permanent magnet. The helical robot is actuated in a viscous fluid characterized by low-Re using rotating magnetic fields produced by a permanent magnet fixed in space by the robotic manipulator. Our experimental results demonstrate the capability to actuate the robot controllably and compensate for its gravity by controlling the angular velocities of the constrained actuator magnet.

As part of future work, we will implement closed-loop control of the helical robot in 3-D space in the presence of position constraint on the actuator magnet. In addition,

we will modify our permanent magnet-based robotic system to actuate the helical robots using two synchronized rotating dipole fields [22]. In the current study, we have demonstrated radial actuation and gravity compensation by the pulling magnetic force of the actuator magnet. To achieve closed-loop motion control in 3-D space, we will mitigate the pulling magnetic forces along the lateral directions of the robots using two synchronized actuating magnets.

REFERENCES

[1] J. Wang and W. Gao, "Nano/Microscale motors: biomedical opportunities and challenges," *ACS Nano*, vol. 6, no. 7, pp. 5745-5751, 2012.

[2] B. J. Nelson, I. K. Kaliakatsos, and J. J. Abbott, "Microrobots for minimally invasive medicine," *Annual Review of Biomedical Engineering*, vol. 12, pp. 55-85, 2010.

[3] A. Hosney, J. Abdalla, I. S. Amin, N. Hamdi, and I. S. M. Khalil, "*In vitro* validation of clearing clogged vessels using microrobots," in *Proceedings of the IEEE RAS/EMBS International Conference on Biomedical Robotics and Biomechatronics (BioRob)*, UTown, Singapore, pp. 272–277, 2016.

[4] M. Sitti, H. Ceylan, W. Hu, J. Giltinan, M. Turan, S. Yim, and E. Diller, "Biomedical applications of untethered mobile milli/microrobots," *Proceedings of the IEEE*, vol. 103, no. 2, pp. 205-224, 2015.

[5] K. E. Peyer, L. Zhang, and B. J. Nelson, "Bio-inspired magnetic swimming microrobots for biomedical applications," *Nanoscale*, vol. 5, no. 4, pp. 1259-1272, 2012.

[6] A. Ghosh and P. Fischer, "Controlled propulsion of artificial magnetic nanostructured propellers," *Nano Letters*, vol. 9, pp. 2243-2245, 2009.

[7] W. Wang, L. A. Castro, M. Hoyos, and T. E. Mallouk, "Autonomous motion of metallic microrods propelled by ultrasound," *ACS Nano*, vol. 6, no. 7, pp. 6122–6132, 2012.

[8] W. F. Paxton, K. C. Kistler, C. C. Olmeda, A. Sen, S. K. St. Angelo, Y. Cao, T. E. Mallouk, P. E. Lammert, and V. H. Crespi, "Catalytic nanomotors: autonomous movement of striped nanorods," *Journal of the American Chemical Society*, vol. 126, no. 41, pp. 13424–13431, 2004.

[9] P. Calvo-Marzal, S. Sattayasamitsathit, S. Balasubramanian, J. R. Windmiller, C. Dao, and J. Wang, "Propulsion of nanowire diodes," *Chemical Communications*, vol. 46, no. 10, pp. 1623–1624, 2010.

[10] J. Lapointe and S. Martel, "Thermoresponsive hydrogel with embedded magnetic nanoparticles for the implementation of shrinkable medical microrobots and for targeting and drug delivery applications," in *Proceedings of the Annual International Conference of the IEEE Engineering in Medicine and Biology Society*, pp. 4246–4249, 2009.

[11] S. Palagi, A. G. Mark, S. Y. Reigh, K. Melde, T. Qiu, H. Zeng, C. Parmeggiani, D. Martella, A. Sanchez-Castillo, N. Kapernaum, F. Giesselmann, D. S. Wiersma, E. Lauga, and P. Fischer, "Structured light enables biomimetic swimming and versatile locomotion of photoresponsive soft microrobots," *Nature Material*, vol. 15, pp. 647–653, 2016.

[12] J. Li, T. Li, T. Xu, M. Kiristi, W. Liu, Z. Wu, and J. Wang, "Magneto–Acoustic hybrid nanomotor," *Nano Letters*, vol. 15, pp. 4814–4821, 2015.

[13] A. W. Mahoney and J. J. Abbott, "Managing magnetic force applied to a magnetic device by a rotating dipole field," *Applied Physics Letters*, vol. 99, 2011.

[14] W. Jing, N. Pagano, and D. J. Cappelleri, "A tumbling magnetic microrobot with flexible operating modes," in *Proceedings of the IEEE International Conference on Robotics and Automation (ICRA)*, Karlsruhe, Germany, pp. 5514–5519, 2013.

[15] E. M. Purcell, "Life at low Reynolds number," *American Journal of Physics*, vol. 45, no. 1, pp. 3-11, 1977.

[16] M. P. Kummer, J. J. Abbott, B. E. Kratochvil, R. Borer, A. Sengul, and B. J. Nelson, "OctoMag: An Electromagnetic System for 5-DOF Wireless Micromanipulation," in IEEE Transactions on Robotics, vol. 26, no. 6, pp. 1006-1017, 2010.

[17] A. W. Mahoney, D. L. Cowan, K. M. Miller, and J. J. Abbott, "Control of untethered magnetically actuated tools using a rotating permanent magnet in any position," in *Proceedings of the IEEE International Conference on Robotics and Automation (ICRA)*, pp. 3375-3380, 2012.

[18] S. Tognarelli, V. Castelli, G. Ciuti, C. Di Natali, E. Sinibaldi, P. Dario, and A. Menciassi, "Magnetic propulsion and ultrasound tracking of endovascular devices," *Journal of Robotic Surgery*, vol. 6, no. 1, pp. 5–12, 2012.

[19] A. W. Mahoney and Jake J. Abbott, "Five-degree-of-freedom manipulation of an untethered magnetic device in fluid using a single permanent magnet with application in stomach capsule endoscopy," *the International Journal of Robotics Research*, vol. 35, no. 1-3, pp. 129–147, 2016.

[20] R. M. Murray, Z. Li, and S. S. Sastry (1994). A Mathematical Introduction to Robotic Manipulation, 1st edn, CRC Press Inc., Boca Raton, FL, USA.

[21] T. Xu, Y. Guan, J. Liu, and X. Wu, "Image-Based visual servoing of helical microswimmers for planar path following," *IEEE Transactions on Automation Science and Engineering*, vol. 17, no. 1, pp. 325–333, 2020.

[22] A. Hosney, A. Klingner, S. Misra, and I. S. M. Khalil, "Propulsion and steering of helical magnetic microrobots using two synchronized rotating dipole fields in three-dimensional space," in *Proceedings of the IEEE/RSJ International Conference on Intelligent Robots and Systems (IROS)*, Rome, Italy, pp. 1988-1993, 2012.

APPENDIX A: DENAVIT-HARTENBERG PARAMETERS OF THE ROBOTIC MANIPULATOR

The Denavit-Hartenberg parameters of the robotic manipulator are provided in Table I. The homogeneous transformation matrix, $\mathbf{T}_{\mathrm{b}}^{0}$, describes the transformation from the base frame of the robotic manipulator to the rotating permanent magnet that is attached to the end-effector. This magnet produces the required magnetic field, $\mathbf{B}$, at position $\boldsymbol{p}$ relative to the helical microrobot, such that

$$\mathbf{T}_{\mathrm{b}}^{0} = \mathbf{T}_{6}^{0}(\boldsymbol{q})\mathbf{T}_{\mathrm{M}}^{6}(\boldsymbol{q}_{\mathrm{M}})\mathbf{T}_{\mathrm{b}}^{\mathrm{M}}(\boldsymbol{r}, \mathbf{M}) \tag{13}$$

where $\mathbf{T}_{6}^{0}(\boldsymbol{q})$ is the homogeneous transformation matrix of the robotic manipulator from the joint space coordinates $\boldsymbol{q} = [\theta_1, \ldots, \theta_6]$ to the Cartesian coordinates of the end-effector. Further, $\mathbf{T}_{\mathrm{M}}^{6}$ is the transformation from the permanent magnet to the end-effector's position. Finally, the transformation $\mathbf{T}_{\mathrm{b}}^{\mathrm{M}}(\boldsymbol{r}, \mathbf{M})$ maps the distance $\boldsymbol{r}$ to a location $\boldsymbol{p}$ and magnetization vector $\mathbf{M}$ to the magnetic field in the desired location.

TABLE I: The Denavit-Hartenberg parameters of the manipulator are used in Equation (13) to determine $\mathbf{M}$ in the mapping (12).

q_i	θ	α	a [mm]	d [mm]	$\theta_{\min}$	$\theta_{\max}$
q_1	0°	0	0	400	-170°	170°
q_2	0°	-90°	25	0	-190°	45°
q_3	$\theta_3 - 90^\circ$	0	560	0	-120°	156°
q_4	θ_4	-90°	25	515	-185°	185°
q_5	θ_5	90°	0	0	-120°	120°
q_6	$\theta_6 + 180^\circ$	-90°	0	90	-350°	350°